PAPER REF: 4718

MECHANICAL BEHAVIOR OF A TUBULAR COMPOSITE STRUCTURE UNDER THE EFFECTS OF A COMBINED LOADING

Mansur Celebi[1(*)], **Halit S. Turkmen**[2]
[1]Aeronautics and Space Technologies Institute, Turkish Air Force Academy, Istanbul, Turkey
[2]Faculty of Aeronautics and Astronautics, Istanbul Technical University, Istanbul, Turkey
[(*)]*Email:* mcelebi@hho.edu.tr

ABSTRACT

In this study, a numerical analysis of a tubular Carbon/Epoxy laminated composite structure under the effect of combined axial and torsional loading is performed. For this purpose the finite element model of the tubular composite is constructed. The effect of fiber orientations and stacking sequence is investigated. The Tsai-Wu strength index, displacement, strain and stress results are obtained for all loading cases. The results are evaluated by using a failure model. The failure is found to be dependent on the fiber orientation angle and ply stacking sequence.

Keywords: tubular composite, combined loading, mechanical behavior, fiber orientation, Tsai-Wu.

INTRODUCTION

Composite materials have many advantages when compared to metallic structures and therefore become inevitable for many industrial applications. Composite materials have better mechanical properties like high specific stiffness, high specific strength, high fatigue strength, and good impact properties. They can be manufactured as smart materials which can be used in structural health monitoring systems with the help of embedded sensors. In addition, they offer higher corrosion and chemical resistance, better dimensional stability and design flexibility over metallic materials. On the other hand the manufacture cost of the composite materials is high and manufacturing high quality composite material depends on the experience.

Composite materials are used in wide variety of applications. Composite tubes with uniform circular cross-section can be used in drive shafts because of extra stiffness. Especially, in aerospace industry it is widely used because of its lightweight and high strength and high fatigue strength. In aerospace composites, like carbon fiber reinforced polymer (CFRP) composites, have the ability to replace aluminum alloys since they weigh less per unit of strength.

Composite materials are being used for decades in transport aircraft components, but, they are mostly used in wing edges or control surfaces. In recent years, the use of composites is extended to the fuselage and wings because of its lightweight and resistance to corrosion compared to the metallic materials that have traditionally been used in aircraft. Not only will the use of composites help save the weight but there will be benefits to the passengers as well. Due to the properties of composites, airlines will be able to increase cabin pressure and increase the cabin humidity which will increase the comfort and prevent jet lag. (Johnson, 2012)

The Boeing 787 is about 50 percent composite by weight and soon it is followed by the Airbus A350, having composite material roughly in the same proportion as dreamliner as shown in the Fig.1.(Freissinet, 2011). However, The Airworthiness Authorities (e.g: FAA in US, EASA in Europe) have some safety concern due to the use of large percentage of composite materials, that its mechanical behavior is still under investigation.

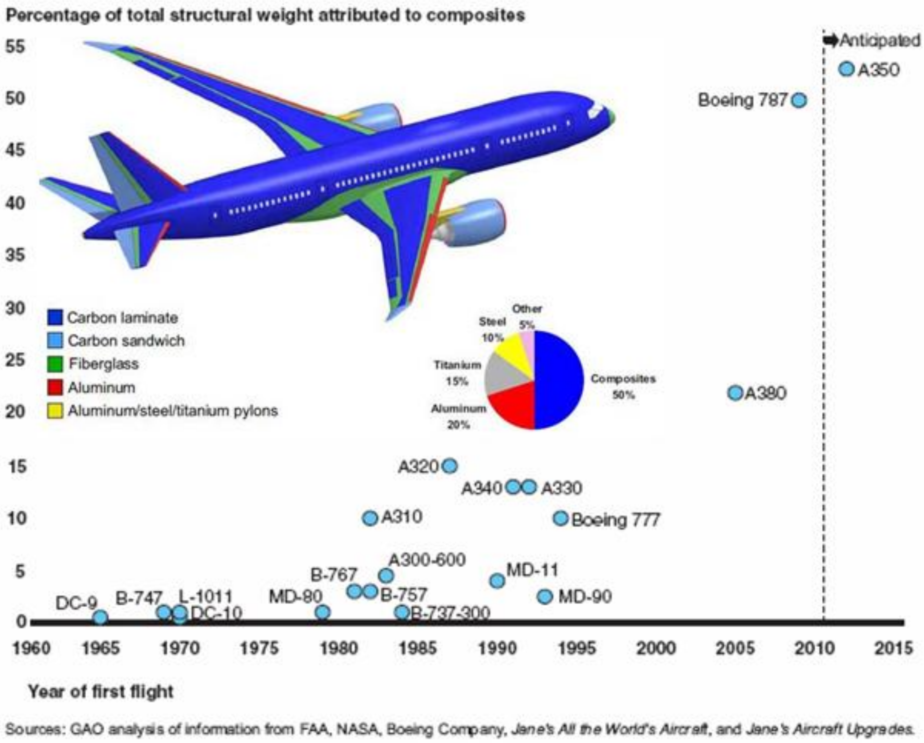

Fig.1. Commercial airplane models over time by percentage of composite and material used in the Boeing 787(Freissinet, 2011)

Therefore in this study tubular cylindrical CFRP composite is selected to model the airframe as shown in the Fig.2.

Figure.2. A Boeing 787 frame, tubular cylinder composite (Freissinet, 2011)

The behavior of composite materials under axial cyclic stress states has been studied for the purpose of developing methodologies for safe fatigue assessments. However, the mechanical behavior under combined loading has been far less investigated, despite its importance in the design of structural components (Quaresimin, 2010). Levi et al. tested CFRP composite tubes under tensile axial loading up to failure and evaluated strength properties as well as failure mechanisms (Levi, 1995). A Through Process Modelling (TPM) methodology proposed by Klimkeit et al. dedicated to the fatigue life assessment of composite required the FE stress–strain analysis (Klimkeit, 2011). Benamira et al. study shows that in the composite tube the plane of failure was in line with the principal direction and under several loading conditions, the small damage undergone by the tubular samples was followed by brittle failure (Benamira, 2011).

In this study, a numerical model is developed to determine the Tsai-Wu strength index, stress and strain distributions within a tubular composite structure under combined torsional and tensile loading to simulate the loading that an airframe is subjected to. For this purpose the finite element model of the tubular cylindrical composite is constructed. The structure is modeled using laminated shell elements. The material is chosen as carbon/epoxy. The finite element model is constructed using ANSYS finite element code. The effect of fiber orientation angle and stacking sequence is investigated. The fiber orientation cases of under combined axial and torsional loading are examined. The displacement, strain and stress results in addition to Tsai-Wu strength index are obtained for all fiber orientation cases. The results are evaluated by using the Tsai-Wu failure model. The failure is found to be dependent on the fiber orientation angle and ply stacking sequence.

FINITE ELEMENT MODELING OF TUBULAR COMPOSITE STRUCTURE

The ANSYS finite element method was used to analyze the model for each fiber orientation and loading case. The goal of this investigation is to study mechanical behavior of a tubular cylindrical geometry of carbon composite structure. An 8-node SHELL281 (Finite Strain Shell) element with six degrees of freedom at each node is selected. The element is suitable for analyzing thin to moderately-thick shell structures and is appropriate for linear, large rotation, and/or large strain nonlinear applications. The area meshing is applied on the surface to model hollow tubular cylindrical composite structure. In the model there are 13089 nodes and 4363 elements.

The average diameter of the tubular cylindrical composite is 25 mm. The length of the composite structure is chosen as 25 cm which is 10 times the average diameter as shown in the Fig.3. This dimension ratio is a typical slenderness ratio for a commercial aircraft.

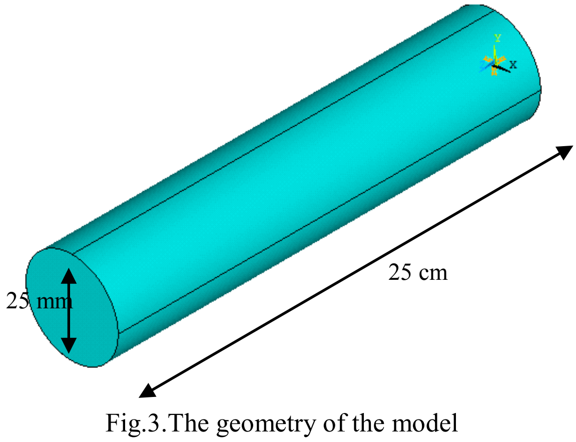

Fig.3.The geometry of the model

The carbon fiber composite model is established from six layers of IM6/3501-6 graphite/epoxy lamina with a nominal thickness of 0.188 mm. The material properties are given in Table 1. (Krueger, 2000)

Table1 Material Properties for IM6/3501-6 Carbon Fiber Lamina

	Lamina
Longitudinal Modulus E_1 GPa	144.7
Transverse Modulus E_2 GPa	9.65
Through Thickness Modulus E_3 GPa	9.65
In-plane Shear Modulus G_{12} GPa	5.2
Transverse Shear Modulus G_{23} GPa	3.4
Transverse Shear Modulus G_{13} GPa	5.2
In-plane Poisson's Ratio ν_{12}	0.30
Through Thickness Poisson's Ratio ν_{23}	0.45
Through Thickness Poisson's Ratio ν_{13}	0.30
Longitudinal Tensile Strength X_T MPa	1950
Longitudinal Compressive Strength X_C MPa	1480
Transverse Tensile Strength Y_T MPa	61
Transverse Compressive Strength Y_C MPa	200
Through Thickness Tensile Strength Z_T MPa	61
Through Thickness Compressive Strength Z_C MPa	200
In-plane Shear Strength S_{12} MPa	79
Transverse Shear Strength S_{23} MPa	79
Transverse Shear Strength S_{13} MPa	79

The finite element model of the tubular cylindrical composite is shown in Fig.4. One end of the structure is fixed and axial, torsional and combined axial-torsional load configurations are applied at the free end. 30 kN axial load is applied in the global z direction and 125 Nm torsional load is applied as shown in the Fig.4.

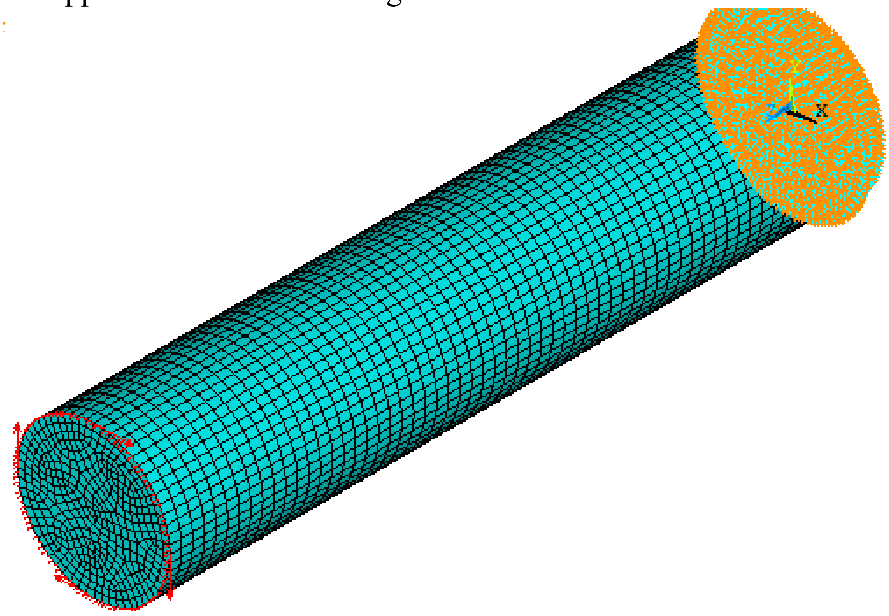

Fig.4.The finite element model of the tubular cylindrical composite with boundary condition and applied loads

Fiber Orientations

The fiber orientations in local coordinate system are shown in the Fig.5 and the results are calculated according to global cylindrical coordinate system.

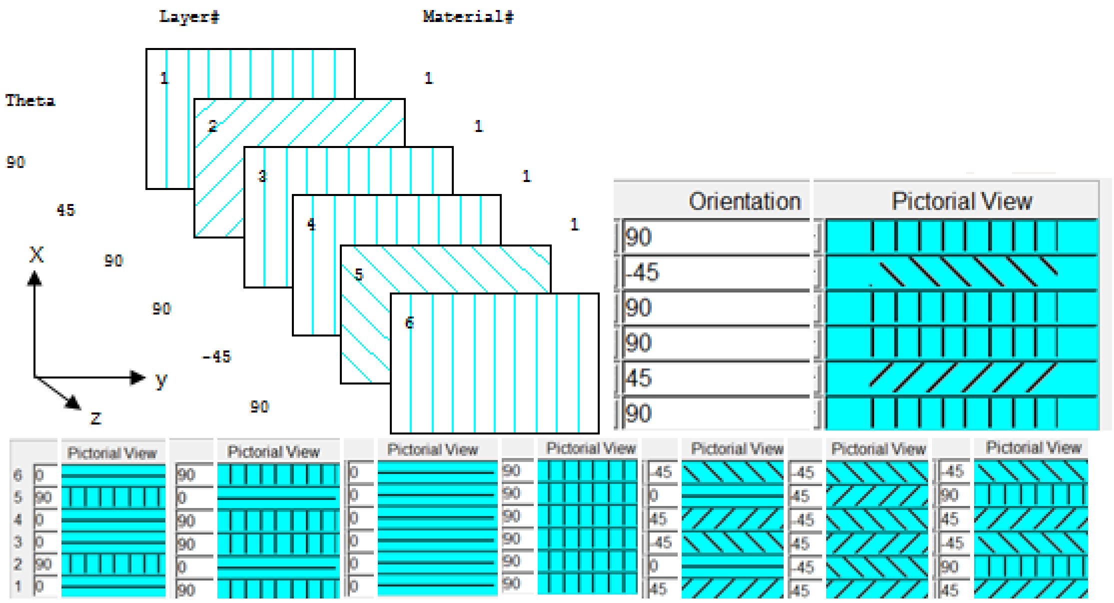

Fig.5. Fiber orientations angles and ply stacking sequence.

FAILURE ANALYSIS

For composite materials one of the important failure theories is Tsai-Wu failure theory. Tsai-Wu theory for anisotropic materials in tensor form states that for composite laminates the failure criteria is as follows.

$$\boldsymbol{F_i\sigma_i + F_{ij}\sigma_i\sigma_j \leq 1} \qquad i,j=1,2,3,4,5,6$$

where *Fi* and *Fij* are strength tensors found through experimental procedures and are related to failure strengths in principal lamina directions. The Tsai-Wu criteria can be used with the 3D composite shell element. These models require both compressive and tensile failure strengths, F_{ijt} and F_{ijc}, to be defined in the plane of the shell which are combined to give a bulk failure criteria. For an orthotropic lamina subjected to plane stress ($\sigma_3 = \tau_{13} = \tau_{23} = F_4 = F_5 = F_6 = F_{16} = F_{26} = 0$) Tsai–Wu failure criterion reduces to as follows;

$$\boldsymbol{F_1\sigma_1 + F_2\sigma_2 + F_{11}\sigma_1^2 + F_{22}\sigma_2^2 + F_{66}\tau_6^2 + 2F_{12}\sigma_1\sigma_2 \leq 1} \quad \text{(Tsai and Wu, 1971)}$$

It is possible to define the parameters from simple test procedures. If the failure strength in uniaxial tension and compression in the two directions of anisotropy are: $\boldsymbol{\sigma_{1t}}$, $\boldsymbol{\sigma_{1c}}$, $\boldsymbol{\sigma_{2t}}$, $\boldsymbol{\sigma_{2c}}$

Then the coefficients of the orthotropic Tsai–Wu failure criterion are:

$$\boldsymbol{F_1=(1/\sigma_{1t}) - (1/\sigma_{1c})\ ; \quad F_1=(1/\sigma_{2t}) - (1/\sigma_{2c})\ ; \quad F_{11}=1/\sigma_{1t}\,\sigma_{1c}\ ; \quad F_{22}=1/\sigma_{2t}\,\sigma_{2c}\ ;}$$

$$\boldsymbol{F_{66}=1/\tau^2_{12}\ ; \quad F_{12}=-1/2(F_{11}*F_{22})^{-1/2}}$$

The Tsai-Wu failure criteria in ANSYS program uses negative values for compression limits, whereas Tsai uses positive values for all limits. Therefore, we may have some negative Tsai-Wu Strength Indexes in the results.

NUMERICAL RESULTS

For the failure investigation the peripheral nodes close to the free end are selected. They are shown in Fig. 6. The failure is investigated by using the Tsai-Wu failure criteria. For given fiber orientation angles; under the combined axial and torsional loading, the maximum values of the Tsai-Wu strength index, displacements and stress and strain values of nodes shown in Fig. 6 are given in Table 2. The lowest Tsai-Wu index value is in [90/45/90/90/-45/90] fiber orientation angle. This shows that compare to other fiber orientation angles, [90/45/90/90/-45/90] fiber orientation shows the best mechanical properties. Whereas [0/0/0/0/0/0] fiber orientation has the highest Tsai-Wu index, axial and radial displacements and axial strains.

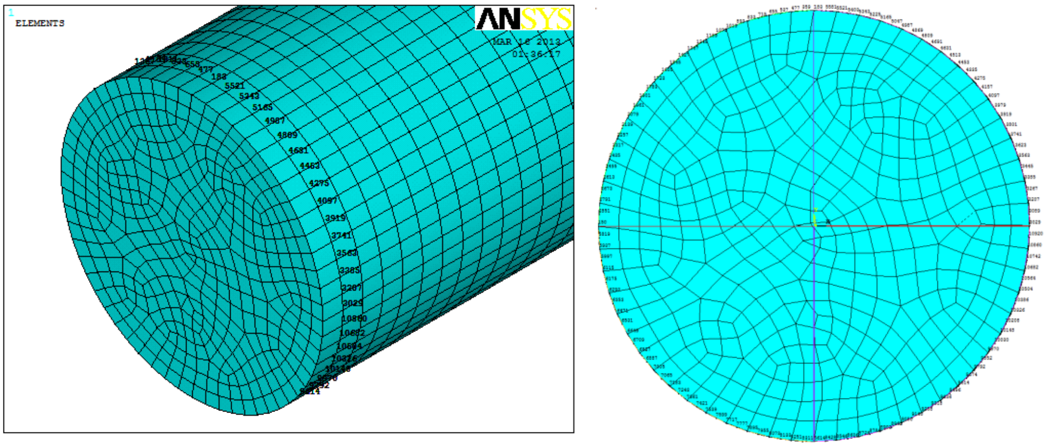

Fig. 6 The selected nodes for failure investigation

Table 2 Maximum values of The Tsai-Wu Strength Index, displacements, stress and strain values under combined axial and torsional loading.

	Fiber Orientation Angle	Tsai-Wu Strength Index	Axial Displ.	Radial Displ.	Axial Stress	Radial Stress	Axial Strain	Radial Strain
1	**0/90/0/ 0/90/0**	1.217	0.720E-03	-0.268E-02	0.578E+08	0.308E+09	0.575E-02	0.203E-02
2	**90/0/90/ 90/0/90**	0.543	0.398E-03	-0.266E-02	0.548E+09	0.295E+08	0.374E-02	0.230E-02
3	**0/0/0/ 0/0/0**	3.866	0.405E-02	-0.270E-02	0.220E+09	0.402E+09	0.225E-01	0.250E-02
4	**90/90/90/ 90/90/90**	0.423	0.281E-03	-0.266E-02	0.509E+09	0.529E+08	0.341E-02	0.536E-02
5	**45/0/-45/ 45/0/-45**	0.684	0.150E-02	-0.514E-03	0.608E+09	0.477E+09	0.113E-01	0.173E-02
6	**45/-45/ 45/ -45/ 45/-45**	0.720	0.209E-02	-0.373E-03	0.600E+09	0.438E+09	0.122E-01	0.209E-02
7	**45/90/-45/ 45/90/-45**	0.354	0.640E-03	-0.519E-03	0.548E+09	0.474E+09	0.666E-02	0.272E-02
8	**90/45/90/ 90/-45/90**	0.155	0.384E-03	-0.867E-03	0.646E+09	0.394E+08	0.445E-02	0.335E-02

Since [90/45/90/90/-45/90] fiber orientation shows the best mechanical properties, it is selected for further investigation. For the tubular cylindrical carbon epoxy composite structure under combined axial and torsional loading; the Tsai-Wu strength index distribution is shown in Fig. 7, the displacement distributions in the axial and radial direction are shown in Fig. 8 and Fig. 9, the stress and strain distributions are shown in Fig. 10, 11, 12 and 13. The results given here are from the top layer of the laminates with the fiber orientation [90/45/90/90/-45/90] which is found to have the lowest Tsai-Wu strength index compare to other fiber orientations.

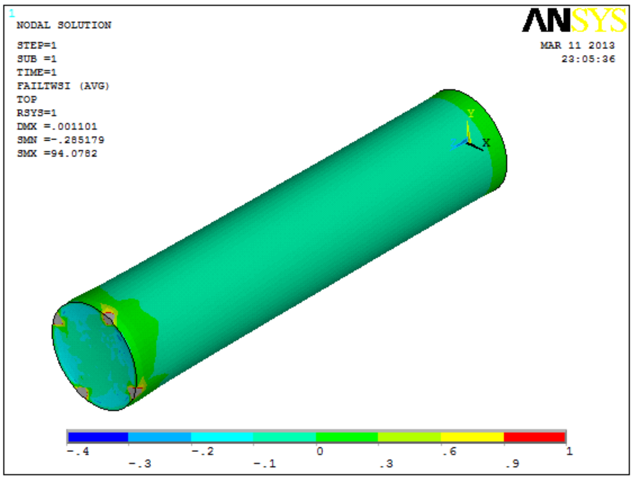

Fig.7 The Tsai-Wu Strength Index Distribution of [90/45/90/90/-45/90] fiber orientation.

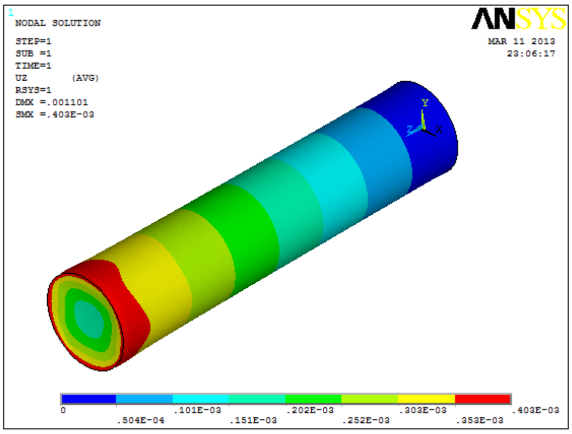

Fig.8 The displacement in the axial direction of [90/45/90/90/-45/90] fiber orientation

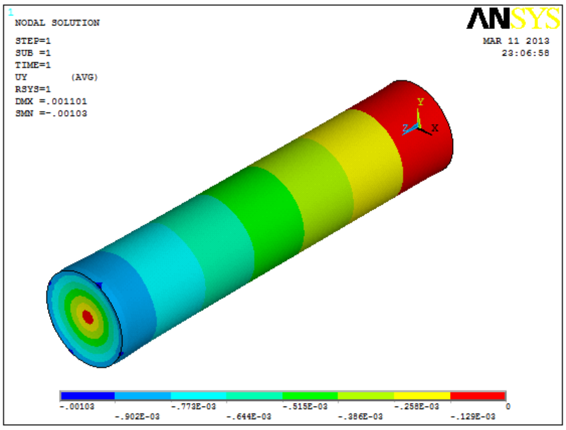

Fig.9 The radial displacement of [90/45/90/90/-45/90] fiber orientation

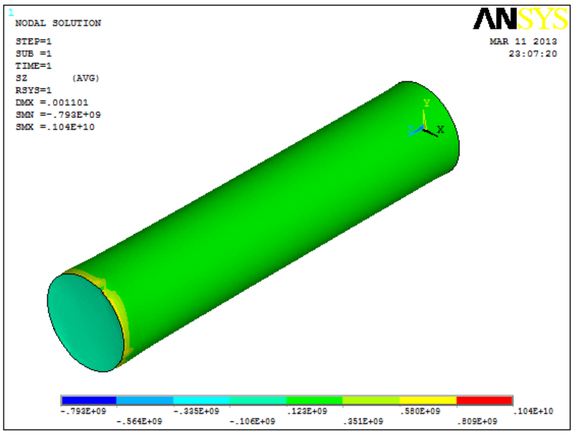

Fig.10 Axial Stress Distribution of [90/45/90/90/-45/90] fiber orientation

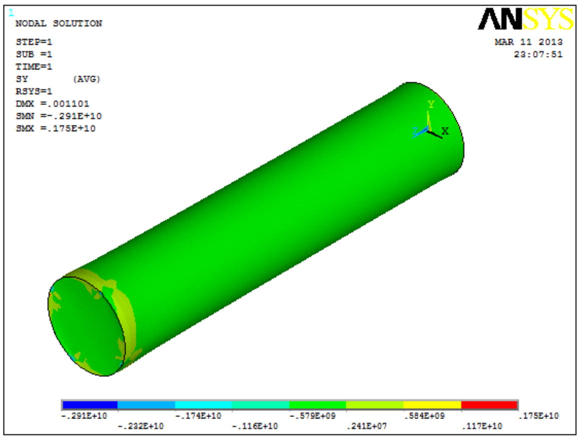

Fig.11 Radial Stress Distribution of [90/45/90/90/-45/90] fiber orientation

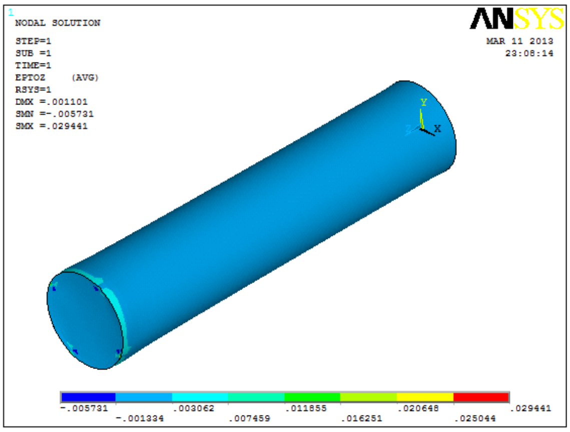

Fig.12 Axial Strain Distribution of [90/45/90/90/-45/90] fiber orientation

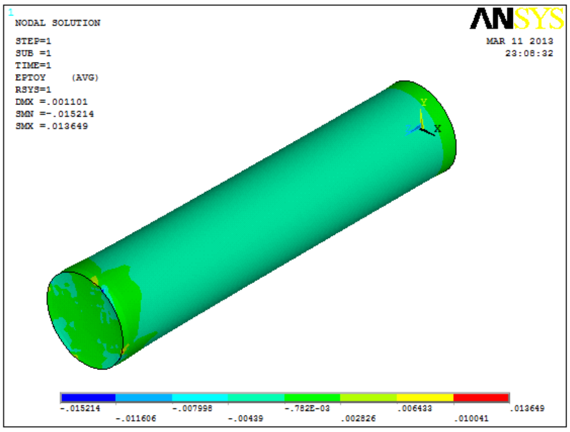

Fig.13 Radial Strain Distribution of [90/45/90/90/-45/90] fiber orientation

When combined axial and torsional loading is applied the Tsai-Wu Strength Index results are varying as shown in Fig. 14 for different fiber orientations. This variation repeats itself in every quarter, which is due to torsional loading in each quarter.

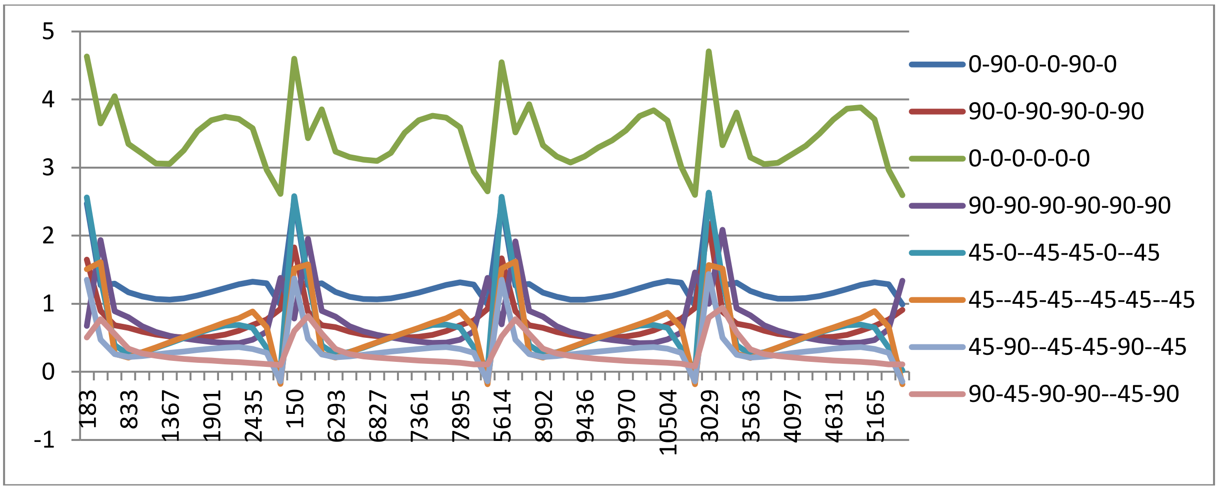

Fig. 14 Tsai-Wu Stength Index under combined loading

The Tsai-Wu Strength Index for 30 kN axial, 125 Nm torsional and combined 30 kN axial-125 Nm torsional loading for different fiber orientations are given in Fig. 15.

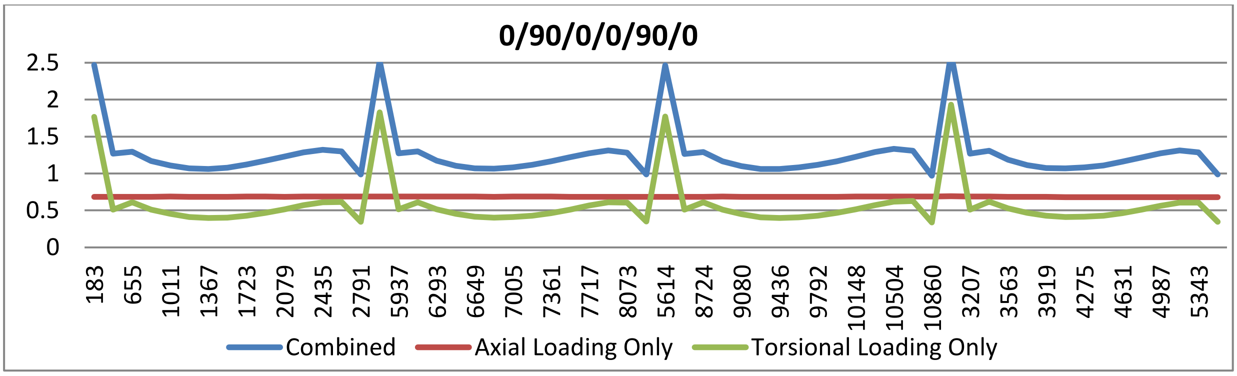

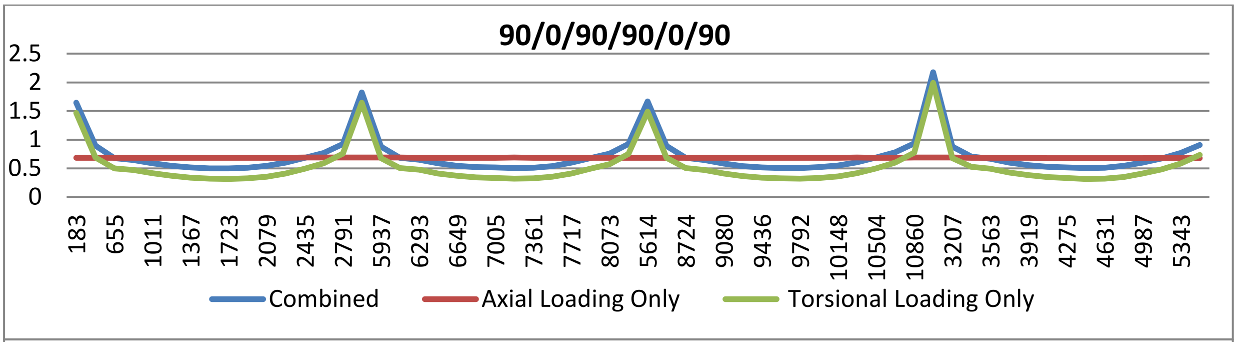
90/0/90/90/0/90
2.5
2
1.5
1
0.5
0
183 655 1011 1367 1723 2079 2435 2791 5937 6293 6649 7005 7361 7717 8073 5614 8724 9080 9436 9792 10148 10504 10860 3207 3563 3919 4275 4631 4987 5343
Combined
Axial Loading Only
Torsional Loading Only

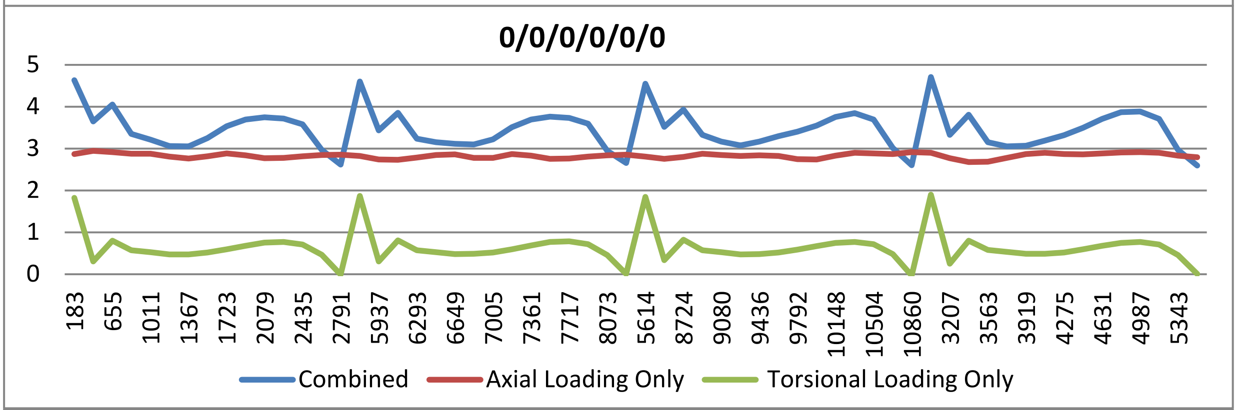
0/0/0/0/0/0
5
4
3
2
1
0
183 655 1011 1367 1723 2079 2435 2791 5937 6293 6649 7005 7361 7717 8073 5614 8724 9080 9436 9792 10148 10504 10860 3207 3563 3919 4275 4631 4987 5343
Combined
Axial Loading Only
Torsional Loading Only

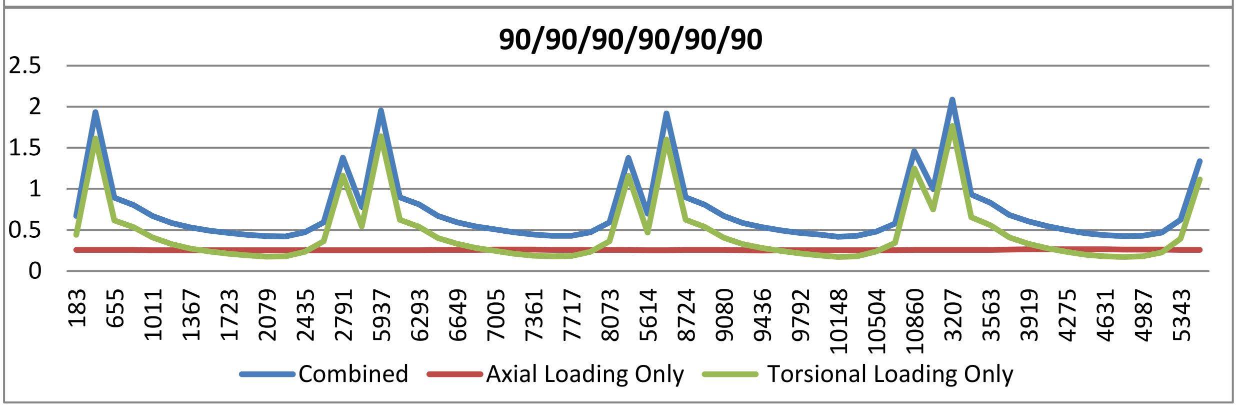
90/90/90/90/90/90
2.5
2
1.5
1
0.5
0
183 655 1011 1367 1723 2079 2435 2791 5937 6293 6649 7005 7361 7717 8073 5614 8724 9080 9436 9792 10148 10504 10860 3207 3563 3919 4275 4631 4987 5343
Combined
Axial Loading Only
Torsional Loading Only

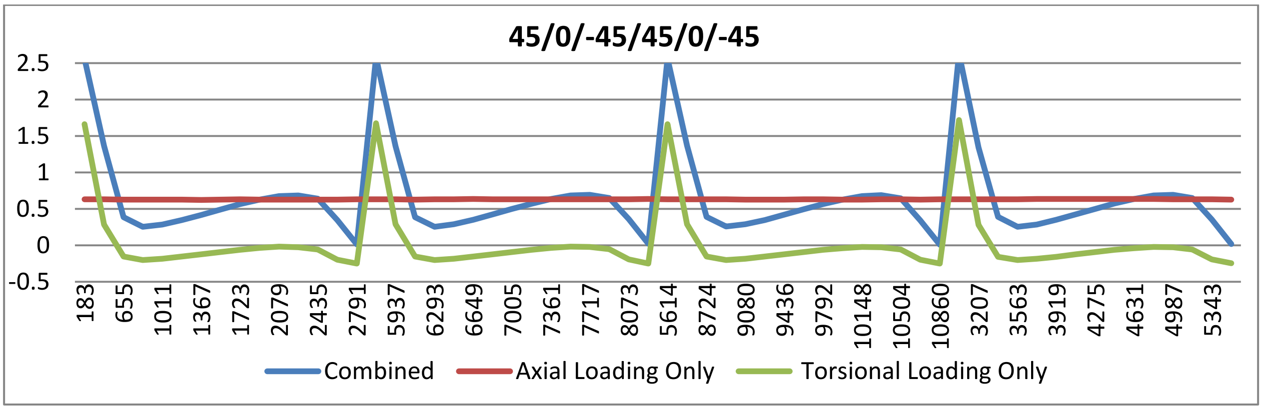
45/0/-45/45/0/-45
2.5
2
1.5
1
0.5
0
-0.5
183 655 1011 1367 1723 2079 2435 2791 5937 6293 6649 7005 7361 7717 8073 5614 8724 9080 9436 9792 10148 10504 10860 3207 3563 3919 4275 4631 4987 5343
Combined
Axial Loading Only
Torsional Loading Only

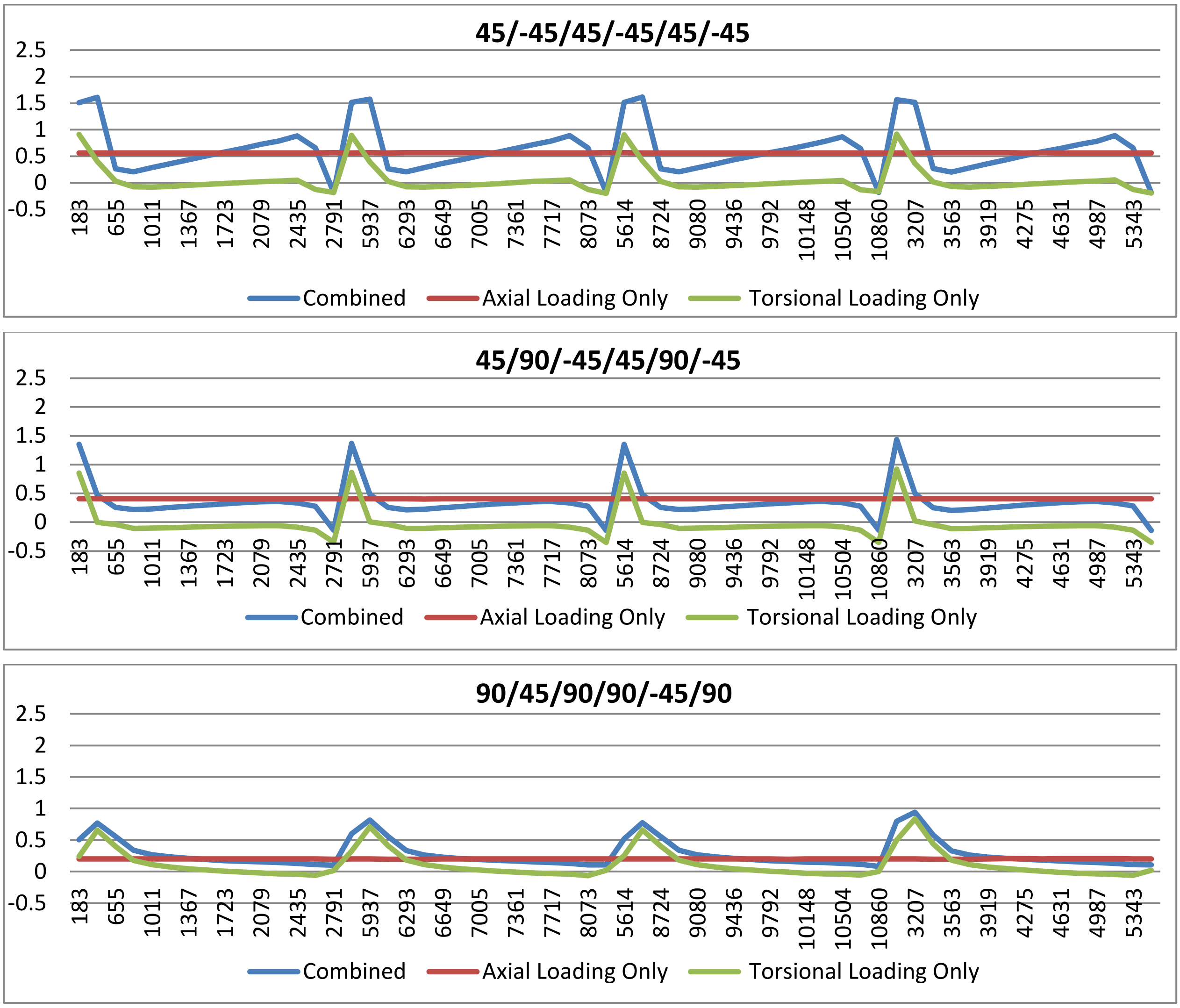

Fig. 15.The Tsai-Wu Strength Index for axial, torsional and combined axial-torsional loading for different fiber orientations

Fig. 15 shows that The Tsai-Wu strength index is higher for axial loading compared to torsional loading for all fiber orientation. However, the strength index values are increasing in the torsional load application points. These results show that, boundary condition effect is very important and must be taken into consideration during analysis.

When we are relatively away from the boundary conditions, which are the midpoints of the model, as shown in Fig. 16, if we investigate [90/45/90/90/-45/90] fiber orientation the Tsai-Wu Strength Index values is less for axial loading and higher for torsional loading which is the inverse of the previous cases. In addition, the boundary conditions effect is very low and the variation is very small. This result is shown in the Fig. 17.

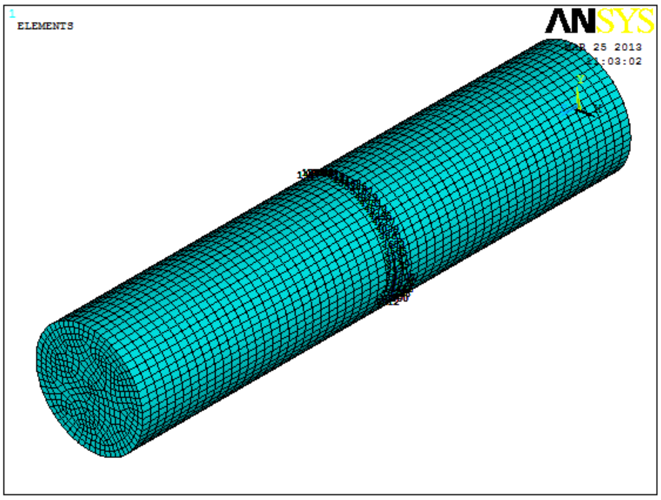

Fig.16 The midpoint nodes

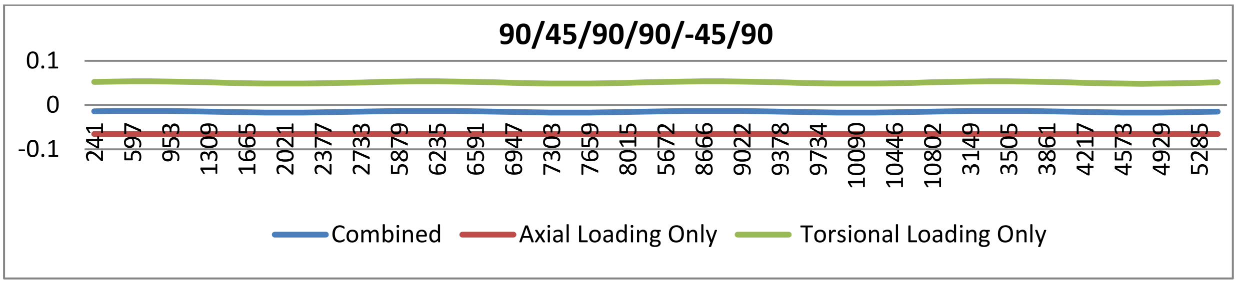

Fig. 17.The Tsai-Wu Strength Index for axial, torsional and combined axial-torsional loading for [90/45/90/90/-45/90] fiber orientation in the midpoint nodes.

The Loading Effect on Tsai-Wu Strength Index

In addition, further investigating the varying loading effect on Tsai- Wu strength index, Fig.18 shows that, for the free end nodes, while increasing the loading the index values are increasing at a higher ratio.

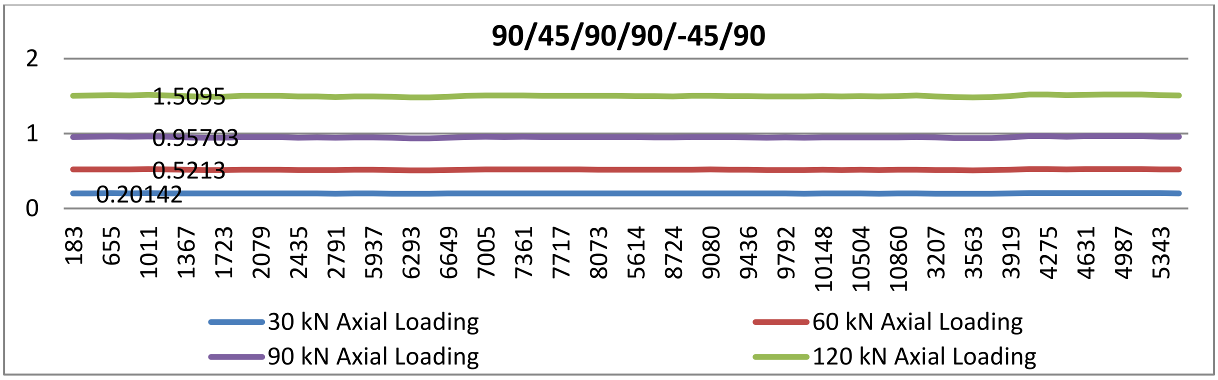

Fig. 18.The Tsai-Wu Strength Index for varying axial loading for [90/45/90/90/-45/90] fiber orientation at the free end nodes.

While we have only axial loading when we double the loading the index value increasing at a rate of 2.6 and then 2.9 which means it has a nonlinear increasing increment ratio. For axial loading the failure does not occur up to loading is increased by three times. After that value the critical Tsai-Wu=1 value is passed and failure occurs.

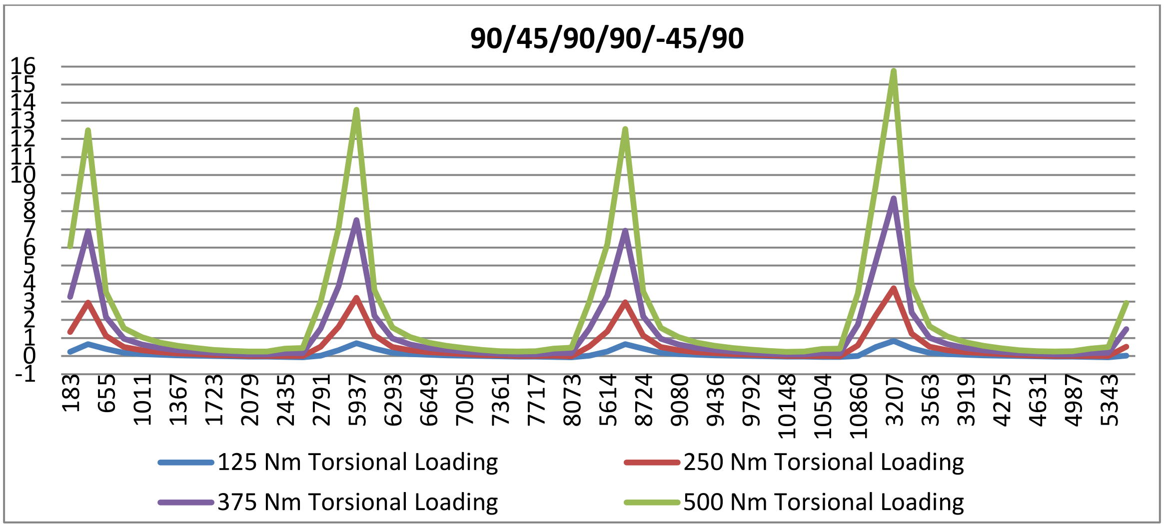

Fig. 19.The Tsai-Wu Strength Index for varying torsional loading for [90/45/90/90/-45/90] fiber orientation at the free end nodes.

When we have torsional loading, Fig. 19 shows that the index value is much higher at the torsional loading application points. However, when we are not in the vicinity of the torsional loading application area the Tsai-Wu index value is very low. Although, the torsional loading is increased four times we are still in the safe side (Tsai-Wu Index≤1) unless we are close to the torsional loading application area.

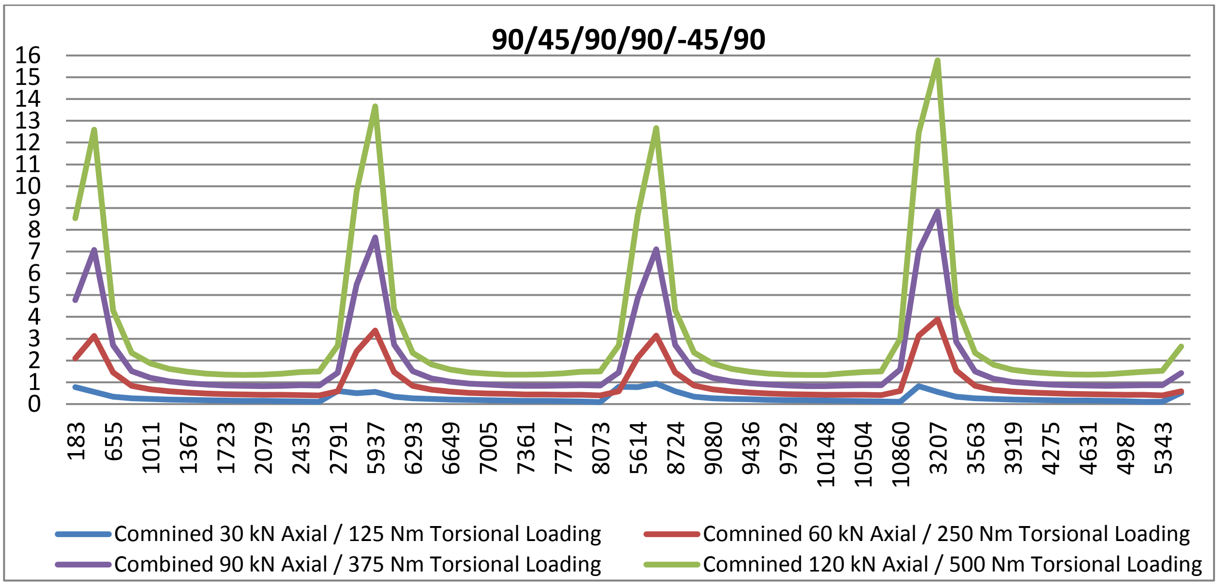

Fig. 20.The Tsai-Wu Strength Index for varying combined axial/torsional loading for [90/45/90/90/-45/90] fiber orientation at the free end nodes.

For combined axial and torsional loading, at the torsional loading application points the critical Tsai-Wu=1 value is passed immediately as shown in Fig. 20 and the highest Tsai-Wu index values occur at node 3207 given in Table 4.

Table 4 Tsai-Wu Strength Index value under varying combined loading

Node 3207				
Axial Loading	**30 kN**	**60 kN**	**90 kN**	**120 kN**
Index value	0,19843	0,51388	0,94637	1,4959

Torsional Loading	**125 Nm**	**250 Nm**	**375 Nm**	**500 Nm**
Index value	0,83544	3,742	8,7196	15,768
Combined Loading	**30 kN Axial/125 Nm**	**60 kN Axial/250 Nm**	**90 kN Axial/375 Nm**	**120 kN Axial/500 Nm**
Index value	0,55872	3,8866	8,8351	15,787

According to Table 4 when combined loading doubled the index value increase by a ratio of 7 and then 4 which means, although the Tsai-Wu index value is very high in the torsional loading application area the increment of the index is decreasing.

CONCLUSIONS

[90/45/90/90/-45/90] ply sequence and the fiber orientations have the highest strength value.

Although the axial loading has higher effect to increase the Tsai-Wu Strength index, the index value in the vicinity of the torsional loading application area is very high which causes the failure.

Since we have only axial and torsional loading the contribution of 0 degree fiber orientation ply to the strength is very low. However, when a thin–walled cylinder is subjected to internal pressure, three mutually perpendicular principal stresses will be set up in the cylinder materials (Circumferential or hoop stress, the radial stress, longitudinal stress). In that case the 0 degree fiber oriented ply would have great contribution.

The boundary condition is very important as it is noticed that the Tsai-Wu strength index is increasing to very high values in the torsional load application points. Therefore, concentrated loading application causes failure immediately.

REFERENCES

Todd Johnson. What Is The 787 Dreamliner. How composite materials make the most advanced airplane ever. About.com,2013. http://composite.about.com/od/applications/a/What-Is-The-787-Dreamliner.htm

Sébastien FREISSINET. Worries about new composite made airplane. 1001crash.com, 2011. http://www.1001crash.com/index-page-composite-lg-2.html

M.Quaresimin, L.Susmel, R.Talreja. Fatigue behaviour and life assessment of composite laminates under multiaxial loadings. International Journal of Fatigue, 32 (2010) 2–16

H.Levi, O.Ishai, E.Altus, I.Sheinman. Mechanical performance of thin-walled tubular composite elements under uniaxial loading part 1: Tensile behaviour. Composite Structures, Volume 31, Issue 2, 1995, p.163-170

B.Klimkeit, Y.Nadot, S.Castagnet, C.Nadot-Martin, C.Dumas, S.Bergamo, C.M.Sonsino, A.Büter. Multiaxial fatigue life assessment for reinforced polymers. International Journal of Fatigue. 33 (2011) 766–780

M.Benamira, C.Hochard, A.Haiahem. Behaviour to failure of fibre mat reinforced composite under combined loading conditions. Composites: Part B 42 (2011) 1412–1419.

Krueger, R., M. K. Cvitkovich, T. K. O'Brien, and P. J. Minguet, "Testing and Analysis of Composite Skin/Stringer Debonding under Multi-Axial Loading," *Journal of Composite Materials*, vol. 34, no. 15, pp. 1263-1300, 2000.

Tsai, S. W. and Wu, E. M. (1971). A general theory of strength for anisotropic materials. Journal of Composite Materials. vol. 5, pp. 58–80.